Optical Switching and Networking 13 (2014) 148–157

Contents lists available at ScienceDirect

Optical Switching and Networking

journal homepage: www.elsevier.com/locate/osn

# Split spectrum-enabled route and spectrum assignment in elastic optical networks

Albert Pagès *, Jordi Perelló, Salvatore Spadaro, Gabriel Junyent

*Universitat Politècnica de Catalunya (UPC), Advanced Broadband Communications Center (CCABA), Barcelona, Spain*

ARTICLE INFO

*Article history:*
Received 27 June 2013
Received in revised form
10 April 2014
Accepted 10 April 2014
Available online 19 April 2014

*Keywords:*
Elastic optical networks
Split spectrum
RSA

ABSTRACT

The Split Spectrum Approach (SSA) in elastic optical networks is based on splitting a demand into smaller sub-signals when a blocking situation arises, either due to the lack of spectral resources or transmission reach reasons. In this paper, we propose a mechanism based on a Mixed Integer Linear Programming (MILP) formulation for efficiently serving incoming demands in SSA-based elastic optical networks. Moreover, we also present a lightweight heuristic mechanism for scenarios where the MILP mechanism may suffer from scalability issues. The benefits of the proposal are highlighted through illustrative results. Furthermore, we compare two SSA implementations available in the literature in terms of relative transponder cost.



## 1. Introduction

In dynamic elastic optical networks [1–3], spectral resources are assigned to incoming demands as a set of contiguous Frequency Slots (FSs), tightly adjusted to their bandwidth needs. However, the random connection arrival and departure process over time and the heterogeneous bandwidth requirements of the demands can lead to high fragmentation of the available optical fiber spectrum [4,5]. This spectrum fragmentation phenomenon arises as a main limitation to successfully serve new incoming demands, since available FSs become scattered along the spectrum in multiple spectral gaps, which complicates the spectrum contiguity constraint to be met.

The recently proposed SSA [6–10] becomes a promising solution to mitigate the pernicious effects of the aforementioned spectrum fragmentation. The rationale behind SSA is as follows: if a demand cannot be allocated due to the lack of enough contiguous FSs in the candidate paths from source to destination, it can be split into multiple lower data-rate sub-signals, which require a smaller number of contiguous FSs and can better fit in the available spectral gaps. As a result, demands that would otherwise be blocked due to the lack of contiguous FSs can eventually be served. Moreover, SSA can be used to avoid demand blocking due to transmission reach reasons, since lower data-rate sub-signals generally support longer transmission distances.

Looking at the literature, SSA can be implemented using multi-flow transponders (referred as MF-TSPs), which allow sending multiple signal flows using a unique device (e.g., see [8,9]), or using multiple bandwidth variable transponders (i.e., BV-TSPs), one per sub-signal after the splitting procedure [10]. Both solutions can apply various strategies to route demand sub-signals (hereafter simply referred as parts) [11–13]: (a) single path strategy, where all parts are routed over the same physical path; (b) multipath strategy, where parts can be routed over different paths. In this paper we follow the single path strategy. Reasons behind this are (a) the avoidance of delay variations among parts, which can lead to packet reordering problems while requiring additional hardware (buffers) at the receiver side, and (b) the reduction of the control plane

* Corresponding author.
*E-mail address:* albertpages@tsc.upc.edu (A. Pagès).

http://dx.doi.org/10.1016/j.osn.2014.04.002
1573-4277/

burden associated to the setup, management and release of the lightpaths supporting the parts.

Although the benefits of SSA have already been highlighted [8,10], no attempts have been made so far (to the best of our knowledge) on addressing the optimal Route and Spectrum Assignment (RSA) in SSA-based dynamic elastic optical networks. Hence, with such a scenario in mind, we present a novel MILP-based mechanism that finds the RSA for incoming demands, minimizing the number of parts into which a demand is split, jointly with the undesired spectrum fragmentation. Using the proposed mechanism, we illustrate the benefits of SSA against conventional elastic optical network scenarios where no demand splitting is enabled. Additionally, we present a lightweight heuristic mechanism capable of producing good solutions in a short time for network scenarios where the scalability of the aforementioned MILP-based mechanism becomes challenged. Furthermore, we also compare CAPEX associated to SSA implementation solutions based on MF-TSPs or BV-TSPs as a function of the relative MF-TSP cost against that of a BV-TSP.

The rest of the paper is structured as follows: Section 2 defines the scenario that we are targeting along with the main assumptions, elaborates on the approach followed to address the RSA problem in a SSA-enabled dynamic elastic optical network and describes the details of the presented mechanisms. Section 3 evaluates the performance of the presented mechanisms through illustrative results and discusses about the mentioned cost analysis. Finally, Section 4 draws up the main conclusions regarding the presented work.

## 2. Efficient RSA with SSA

Without loss of generality, we assume that the data-rate requested by a demand can be translated into a specific bandwidth $B$ in GHz, given the modulation format used to successfully reach the destination. Ideally, the number of FSs needed to serve a demand should be the ceiling of $B$ divided by the width of a single FS, denoted as $F_w$. However, Bandwidth Variable Wavelength Cross Connects (BV-WXCs) require guard bands between demands to properly operate [14]. Let $G$ be the guard band size in GHz, the number of FSs needed to allocate a demand, denoted as $S$, can be calculated as

$$S = \left\lceil \frac{B+G}{F_w} \right\rceil \tag{1}$$

Guard band requirements imposed by BV-WXCs can increase the initial value of $S$, which may be more noticeable when performing SSA. Indeed, the number of FSs needed to allocate a demand split into $M$ parts is

$$S = \sum_{i=1}^{M} \left\lceil \frac{B_i+G}{F_w} \right\rceil \tag{2}$$

where $B_i$ is the amount of $B$ allocated in the $i$th part, that is, $B = \sum_{i=1}^{M} B_i$. Using the mathematical properties of the ceiling function, it can be extracted from (2) that:

$$\left\lceil \frac{B+M\times G}{F_w} \right\rceil + M - 1 \geq S \geq \left\lceil \frac{B+M\times G}{F_w} \right\rceil \tag{3}$$

This relationship serves in determining how many FSs are needed when dividing $B$ in a number of parts $M$, also giving upper and lower bounds of this value. Note, however, that some restrictions apply on the minimum and maximum part size. The minimum size of a part that allows allocating some amount of $B$ is

$$S_{min} = \left\lceil \frac{G+\epsilon}{F_w} \right\rceil \tag{4}$$

where $\epsilon$ denotes an infinitesimal amount of $B$. Otherwise, the part would not be compliant with the guard band requirements when allocating useful demand bandwidth. The maximum size of a part, referred as $S_{max}$, is equal to the number of FSs determined by (1), avoiding to waste spectral resources due to allocating more FSs than needed.

In what follows, a mechanism called Split Spectrum-enabled RSA (SSRSA) is proposed to efficiently allocate incoming demands in SSA-based dynamic elastic optical networks. SSRSA is valid for both SSA implementation strategies using MF-TSPs or BV-TSPs. Note, however, that SSRSA only employs SSA to solve demand blocking due to lack of enough contiguous FSs, as we assume moderately-sized networks where all candidate paths are within the maximum transmission reach of the signals. Additionally, we present a lightweight heuristic mechanism called H-SSRSA for scenarios where scalability could be an issue.

### 2.1. SSRSA mechanism

Let the optical network substrate be characterized by a graph $G_n = (N, E)$, where $N$ denotes the set of nodes and $E = \{(i,j),(j,i): i,j \in N, i \neq j\}$ the set of physical links. Let $F$ denote the set of available FSs per physical link and $d$ the incoming demand to be allocated. We define $P_d$ as the set of candidate paths over $G_n$ for demand $d$, with $h_p$ the length in hops of path $p$, $F_u^p$ as the set of FSs already in use over $p \in P_d$, and $TSP_s$ and $TSP_d$ as the number of unused transponders at source and destination nodes, respectively. Finally, $M_{max}$ denotes the maximum number of parts into which a demand can be split (i.e., to avoid excessive splitting) and $L_{max}$ denotes the maximum number of independent flows a MF-TSP is capable to produce. Regarding the MF-TSP-base implementation, we consider that a single MF-TSP is used to transmit at most one demand, being split or not, with the aforementioned limit of independent flows.

The proposed mechanism executes a MILP formulation, considering the demand needs, the candidate paths and the actual state of the network resources, with the objective of minimizing the number of parts required to allocate $d$, together with the spectrum fragmentation on the network. The aim of the first objective is to reduce the number of required TSPs to serve the demand (BV-TSP-based implementation) as well as the complexity of the whole assignment process since more parts will require a larger control plane burden in terms of setup, management and release operations. Moreover, another reason to encourage the minimization of the number of parts is that, due to the presence of the guard bands, dividing a demand into a large number of parts will usually result in more spectral resources (i.e. FSs) needed to allocate the demand.

As for the second objective, since we are tackling down an online optimization scenario, where demands arrive and depart at random, the aforementioned spectrum fragmentation effect becomes a limiting factor when trying to establish a new connection. Under such scenario, it is desirable to keep the spectrum fragmentation at minimum in order to facilitate the establishment of future demands. The approach that the presented mechanism follows in this respect is to minimize the average end-to-end spectrum fragmentation in the candidate paths for the demand that is being established, since an overall network defragmentation would be too costly to perform. In this regard, the MILP formulation minimizes the contiguous busy portions in the spectrum, that is, it tries to fit the demands so as to avoid having idle spectrum gaps in between occupied resources. Doing so the free spectral resources will become less scattered along the total fiber spectrum, hence, reducing the spectrum fragmentation in the network.

If the model finds a non-empty solution, it means that a feasible RSA for the demand has been found. In this event, resources are reserved and the network status is updated accordingly. Otherwise, the demand is marked as blocked. A pseudo code of the mechanism is depicted in Fig. 1.

Regarding the specific MILP formulation, the model variables are as stated below:

$x_{p,f}$ binary; 1 if slot $f$ is the first slot of a part in path $p$, 0 otherwise.

$y_{p,f}$ binary; 1 if slot $f$ is used in path $p$ to allocate $d$, 0 otherwise.

$z_{p,f}$ binary; 1 if slot $f$ is occupied in path $p$, 0 otherwise.

$u_p$ binary; 1 if path $p$ is used to allocate $d$, 0 otherwise.

$m_p$ integer; number of parts into which $d$ is split that are routed through path $p$.

$s_p$ integer; number of FSs needed to allocate $d$ that are routed through path $p$.

**Inputs:** $d$, $G_n$, $F$, $G$, $F_w$, $K$, $M_{max}$, $L_{max}$, $\alpha$; **Output:** $Sol$

**Phase 1: Pre-processing**
$TSP_s \leftarrow$ free transponders at source node
$TSP_s \leftarrow$ free transponders at destination node
**if** $TSP_s = 0$ **or** $TSP_d = 0$ **then**
  **Demand blocked**
**else**
  $P_d \leftarrow$ K shortest paths in terms of number of hops
  **for** $i = 1$ **to** $K$ **do**
    $F_u^i \leftarrow$ set of end-to-end busy FSs in path $i$
  **Phase 2: MILP solving**
  $Sol \leftarrow$ output from MILP
  **Phase 3: Solution evaluation**
  **if** $Sol = \emptyset$ **then**
    **Demand blocked**
  **else**
    Return $Sol$
    Update network resources according to $Sol$
    **Demand allocated**

**Fig. 1.** SSRSA pseudo-code.

$t_p$ integer; number of busy contiguous spectrum portions in path $p$.

$c$ integer; used to calculate the ceiling function present in Eq. (3)

$v_{p,f,f+1}$, $w_{p,f,f+1}$ real; auxiliary variables $\in$ [0,1].

Before detailing the exact MILP formulation, we first introduce the procedure that is followed to compute $m_p$ in a candidate path. Taking the state of the spectral FSs, a potential part of $d$ is discriminated by a free-to-allocated and another allocated-to-free FS transition, namely, a 0–1 and a 1–0 transition in variables $y_{p,f}$. Thus, we subtract $y_{p,i+1}$ from $y_{p,i}$. If the result is different from 0, a transition is detected. Therefore:

$$m_p = 0.5 \sum_{i=1}^{|F|-1} |y_{p,i} - y_{p,i+1}| \tag{5}$$

However, Eq. (5) does not detect correctly transitions before the initial and after the last FS of the fiber link spectrum. Then, we add $y_{p,1}$ and $y_{p,|F|}$ in (5) to properly compute $m_p$:

$$m_p = 0.5 \left( y_{p,1} + y_{p,|F|} + \sum_{i=1}^{|F|-1} |y_{p,i} - y_{p,i+1}| \right) \tag{6}$$

The term within the sum in (6) can only take values equal to $-1$, 0 or 1. Then, we can substitute the absolute value function by the square function, which results in:

$$m_p = 0.5 \left( y_{p,1} + y_{p,|F|} + \sum_{i=1}^{|F|-1} (y_{p,i}^2 - 2y_{p,i}y_{p,i+1} + y_{p,i+1}^2) \right) \tag{7}$$

Thanks to the binary nature of the variables, quadratic terms can be simplified. Thus, rearranging expression (7):

$$m_p = \sum_{i=1}^{|F|} y_{p,i} - \sum_{i=1}^{|F|-1} y_{p,i}y_{p,i+1} \tag{8}$$

Using expression (8) we obtain the number of parts into which $d$ is split and is routed through path $p$. A similar reasoning can be applied to obtain the number of busy contiguous spectral portions in a candidate path (i.e., considering variables $t_p$ and $z_{p,f}$). However, a product of decision variables is encountered, making the expression non-linear. To linearize it, auxiliary variables $v_{p,f,f+1}$ and $w_{p,f,f+1}$ are introduced, together with some additional constraints in the proposed MILP formulation, which is detailed in what follows:

$$\min \alpha \frac{1}{M_{max}|P_d|} \sum_{p \in P_d} h_p m_p + (1-\alpha) \frac{2}{|P_d||F|} \sum_{p \in P_d} h_p t_p + \epsilon \frac{1}{|P_d||F|} \sum_{p \in P_d} \sum_{i=1}^{|F|} i h_p y_{p,i} \tag{9}$$

subject to:

$$\frac{B + \sum_{p \in P_d} m_p \times G}{F_w} + 1 \geq c \geq \frac{B + \sum_{p \in P_d} m_p \times G}{F_w} \tag{10}$$

$$c + \sum_{p \in P_d} m_p - 1 \geq \sum_{p \in P_d} s_p \geq c \tag{11}$$

$$\sum_{p \in P_d} s_p \geq S_{min} \times \sum_{p \in P_d} m_p \tag{12}$$

$$\sum_{j=i}^{i+S_{max}} y_{p,j} \le S_{max}, \quad \forall p \in P_d, \ \ i = 1, \ldots, |F| - S_{max} \tag{13}$$

$$\begin{aligned} & x_{p,i} \le y_{p,j}, \quad \forall p \in P_d, \ \ i = 1, \ldots, |F| - S_{min} + 1 \\ & \qquad j = i, \ldots, i + S_{min} - 1 \\ & \qquad x_{p,i} = 0, \quad \forall p \in P_d, \ \ i = |F| - S_{min} + 2, \ldots, |F| \end{aligned} \tag{14}$$

$$y_{p,i-1} \le 1 - x_{p,i}, \quad \forall p \in P_d, \ \ i = 2, \ldots, |F| \tag{15}$$

$$m_p = \sum_{i=1}^{|F|} y_{p,i} - \sum_{i=1}^{|F|-1} v_{p,i,i+1}, \quad \forall p \in P_d \tag{16}$$

$$t_p = \sum_{i=1}^{|F|} z_{p,i} - \sum_{i=1}^{|F|-1} w_{p,i,i+1}, \quad \forall p \in P_d \tag{17}$$

$$\sum_{i=1}^{|F|} x_{p,i} = m_p, \quad \forall p \in P_d \tag{18}$$

$$\sum_{i=1}^{|F|} y_{p,i} = s_p, \quad \forall p \in P_d \tag{19}$$

$$y_{p,f} = 0, \quad \forall p \in P_d, \ \ f \in F_u^p \tag{20}$$

$$\begin{aligned} & z_{p,f} = 1, \quad \forall p \in P_d, \ \ f \in F_u^p \\ & z_{p,f} = y_{p,f}, \quad \forall p \in P_d, \ \ f \in F \backslash F_u^p \end{aligned} \tag{21}$$

$$\begin{aligned} & v_{p,i,i+1} \le y_{p,i}, \quad y_{p,i+1} \\ & v_{p,i,i+1} \ge y_{p,i} + y_{p,i+1} - 1, \quad \forall p \in P_d, \ \ i = 1, \ldots, |F| - 1 \end{aligned} \tag{22}$$

$$\begin{aligned} & w_{p,i,i+1} \le z_{p,i}, \quad z_{p,i+1} \\ & w_{p,i,i+1} \ge z_{p,i} + z_{p,i+1} - 1, \quad \forall p \in P_d, \ \ i = 1, \ldots, |F| - 1 \end{aligned} \tag{23}$$

$$\sum_{p \in P_d} m_p \le TSP_s, \quad TSP_d \tag{24a}$$

$$\sum_{p \in P_d} m_p \le L_{max} \tag{24b}$$

$$\sum_{p \in P_d} m_p \le M_{max} \tag{24c}$$

$$u_p \ge y_{p,f}, \quad \forall p \in P_d, \ \ f \in F \tag{25}$$

$$\sum_{p \in P_d} u_p = 1 \tag{26}$$

Objective function (9) has a twofold goal. First, it minimizes the number of parts into which $d$ is split in order to be served. Moreover, it minimizes the spectrum fragmentation in the candidate paths through the minimization of the number of contiguous busy spectrum portions. Parameter $\alpha \in [0, 1]$ is used for pondering purposes, while the last term in (9) aims to speed up the convergence time of the model, with $\epsilon \ll 1$. The usefulness of the convergence term comes from the fact that, initially, the MILP formulation may find itself with a lot of symmetrical solutions with different RSA which evaluate the objective function to the same value. In such conditions, the MILP formulation will have troubles on deciding an initial root solution for starting the exploration of the solution space. In order to help the MILP formulation making faster decisions when it faces the situation where many different solutions lead to the same objective value, we introduce the convergence factor.

Essentially, it prioritizes the lower part of the spectrum when assigning resources to $d$, so in this way the model will quickly prefer lower indexed slots when there are multiple candidate slots, exploring faster the solution space. Furthermore, the convergence term also helps in providing a solution that requires less spectral resources (i.e., FSs), since the model will try to minimize the summation of the used FSs. Finally, all terms in the objective function are pondered by the length in hops of the associated candidate path ($h_p$). This is done since shorter candidate paths will usually entail using less network resources, hence, helping on having enough free resources for future demands.

Constraints (10) and (11) build the relationship depicted in (3), where variable $c$ is used to calculate the ceiling function that appears in that expression. Constraint (12) adds an additional lower bound for the total number of allocated FSs due to the presence of $S_{min}$, ensuring that the total number of allocated FSs does not fall below the number of used parts multiplied by the minimum size of a part ($S_{min}$). Constraints (13) and (14) bound the minimum and maximum individual part size as presented before. Note that, despite the presence of constraint (12), constraints (14) are still necessary to guarantee that the size of each individual part does not fall below the minimal allowed size part. Constraints (15) set the minimum separation between parts to one FS.

Constraints (16) and (17) account for the number of parts into which $d$ is split and the number of contiguous busy spectrum portions in the candidate paths, respectively. Constraints (18) and (19) are the traffic constraints, accounting for the number of needed FSs. Constraints (20) prevent the use of FSs that are already occupied. Constraints (21) give value to variables $z_{p,f}$ according to the current state of the FSs and the choice made by the model, while constraints (22) and (23) give value to auxiliary variables $v_{p,f,f+1}$ and $w_{p,f,f+1}$.

Constraints (24) set the upper limit of parts into which $d$ may be split. More specifically, constraint (24a) avoids splitting $d$ in more parts than available TSPs at source and destination nodes, constraint (24b) avoids splitting $d$ in more parts than flows a MF-TSP is able to produce, while constraint (24c) sets the upper limit of the allowed number of parts as commented before. Note that the first constraint (24a) is only applied in a BV-TSP-based implementation while the second constraint (24b) is only applied in a MF-TSP-based implementation. As for constraint (24c), it is applied for both MF-TSP and BV-TSP-based implementations.

Finally, constraints (25) and (26) restrict the routing to a unique candidate path. We remind the reader that in this paper we are focusing on the single-path approach, where all parts are routed through the same physical path.

Note that the presented model is based on a link-path formulation, so restricting the size of $P_d$ to $K$ may not lead to obtaining the overall optimal solution. The reason to follow such approach is due to the fact that we are targeting an online optimization problem, so the execution times of the model have to be under a reasonable time threshold. Such

time requirements would not be met if other modeling approaches were to be adopted, such as a flow-based formulation. For this reason, we adopted a link-path-based formulation that allows us to find a trade-off between computational requirements of the model and optimality of the solution found by properly setting the value of $K$.

Moreover, as commented in the beginning of this section, we are tackling the route and spectrum assignment to demands in a SS-enabled elastic network considering that a proper modulation format has already been chosen to reach the destination node. Indeed, in a SS environment, since demands can be split in smaller sub-signals with a lower bit-rate than the original demand, more robust modulation formats can be selected for each one of the resulting parts. In order to tackle the optimal selection of the modulation format, an additional dimension would have to be added to the presented MILP formulation. This new dimension would represent the modulation format space, allowing us to select the most suitable modulation format for every of the parts in terms of bit-rate of the part and spectrum requirements of the modulation format. Such optimization problem would significantly increase its solution space, hence, increasing the complexity of the MILP formulation, so other modeling techniques, e.g., channel-based RSA [15], would have to be adopted to efficiently address the problem. The depiction of such MILP formulation is out of the scope of the current paper and left for further studies.

### 2.2. H-SSRSA mechanism

As it will be shown, although execution times of SSRSA fall in the sub-second range in medium-sized network scenarios, they substantially increase as network resources increase. In light of this, we also present a heuristic called H-SSRSA that has the same objective as SSRSA and can be used in large network scenarios. Based on the heuristic procedure in [10], H-SSRSA comprises the following steps:

1. Check if there is at least one available transponder in both source and destination nodes. Not being the case, mark the demand as blocked.
2. Compute K-shortest candidate paths from source to destination nodes.
3. For each candidate path, check if the total number of available FSs is equal or higher than the minimum number of FSs needed to allocate $d$ (i.e., in a single part). If not, mark the candidate path as infeasible. Otherwise, sort the available spectral gaps in descending order according to the following expression:
$$\alpha\frac{g}{G_{max}}+(1-\alpha)\frac{G_{min}}{g} \quad (27)$$
where $g$ denotes the size of the particular gap and $G_{max}$ and $G_{min}$ the sizes of the largest and smallest gaps in the path, respectively.
4. For each of the feasible candidate paths, start filling the available spectral gaps from the first to the last one, according to the previous ordering, with useful bandwidth of $d$ plus the guard bands (each gap will allocate a part of $d$). If $d$ cannot be completely allocated in the path, or the number of resulting parts exceeds $M_{max}$, or there are not enough TSPs at source/destination nodes to support the resulting RSA (BV-TSP case), or the number of parts exceeds $L_{max}$ (MF-TSP case), mark the path as infeasible.
5. If no feasible candidate path still exists, set $d$ as blocked. Otherwise, evaluate the objective function as in the MILP model particularized for each one of the feasible candidate paths, and choose the path with the smallest value. Take its RSA as the solution of H-SSRSA, reserve the associated network resources and set $d$ as served.

Note that by sorting the available spectral gaps according to (27), the H-SSRSA mechanism tries to replicate the behavior of the SSRSA mechanism. If $\alpha=1$, the available gaps will be ordered from the biggest to the smallest, so once they are filled with useful bandwidth of $d$, the number of parts is being minimized. In the opposite case ($\alpha=0$), the available gaps will be ordered from the smallest to the biggest, so when filling them, the total number of spectral gaps after the filling process is minimized. Any case in between would lead to a trade-off solution between the minimization of the number of parts and the spectral gaps in the candidate path. Indeed, it can be seen that with this ordering, jointly with the evaluation of the same objective function as in the MILP formulation, H-SSRSA pursues the same optimization goal as SSRSA.

## 3. Results and discussion

In this section we evaluate the performance of the SSRSA mechanism. In order to quantify the benefits of optimally splitting demands, we benchmark it to a scenario where no splitting is performed (hereafter referred as 1-SSRSA), forcing $M_{max}=1$ and $\alpha=0$ in the formulation. Two network scenarios have been considered, namely, the EON16 (16 nodes, 23 links) [16] and DT (14 nodes, 23 links) [17] network topologies. Besides, two situations with 160 and 320 FSs per fiber link have been assumed, with $F_w=6.25$ GHz and $G=10$ GHz. Regarding network nodes, we assume them equipped with an infinite pool of TSPs (i.e., no blocking occurs due to the lack of TSPs).

Results have been extracted by generating $10^5$ bidirectional demand requests per execution. Requests arrive to the network following a Poisson process, with exponentially distributed Holding Times (HTs). Loads are thus generated by adjusting the ratio between the mean HT and Inter-Arrival Time (IAT), so that load=HT/IAT. Bandwidth requirements of the demands are uniformly chosen among 32, 64, 96 and 128 GHz. Moreover, $K=3$, $M_{max}=L_{max}=4$ and $\alpha=0.5$ are set in all cases. All simulations are run in standard PCs with i7-3770 CPUs at 3.4 GHz and 16 GB RAM using CPLEX v12.5.

Table 1 displays the percentage of blocked bandwidth (BBw) for 1-SSRSA and SSRSA, as well as the average number of TSPs used per node when either BV-TSPs or MF-TSPs are equipped in network nodes. As seen, SSRSA lowers BBw significantly in contrast to 1-SSRSA. Particularly, we can observe differences of one order of magnitude for low loads in both networks and scenarios, with relative gains no worse than 69% for higher loads. In light

**Table 1**
Performance comparison.

| Scenario | | | 1-SSRSA | | SSRSA | | |
|---|---|---|---|---|---|---|---|
| **Network** | **\|F\|** | **Load** | **% BBw** | **BV-TSPs/node** | **% BBw** | **BV-TSPs/node** | **MF-TSPs/node** |
| EON16 | 160 | 5 | 0 | 0.69 | 0 | 0.69 | 0.69 |
| | | 10 | 0.0108 | 1.3 | 0.0016 | 1.3 | 1.3 |
| | | 15 | 0.1721 | 1.92 | 0.0319 | 1.93 | 1.93 |
| | | 20 | 1.0435 | 2.53 | 0.2499 | 2.58 | 2.55 |
| | | 25 | 3.3271 | 3.09 | 1.0503 | 3.27 | 3.18 |
| | 320 | 30 | 0.0016 | 3.77 | 0 | 3.79 | 3.79 |
| | | 40 | 0.0344 | 5.05 | 0.0039 | 5.06 | 5.06 |
| | | 50 | 0.3627 | 6.28 | 0.0402 | 6.38 | 6.36 |
| | | 60 | 1.86 | 7.54 | 0.244 | 7.67 | 7.55 |
| | | 70 | 4.04 | 8.55 | 1.1244 | 9.21 | 8.79 |
| DT | 160 | 5 | 0 | 0.78 | 0 | 0.78 | 0.78 |
| | | 10 | 0.0152 | 1.5 | 0.0012 | 1.5 | 1.5 |
| | | 15 | 0.1677 | 2.21 | 0.0256 | 2.21 | 2.21 |
| | | 20 | 0.6769 | 2.9 | 0.1716 | 2.94 | 2.93 |
| | | 25 | 2.2554 | 3.57 | 0.6914 | 3.67 | 3.61 |
| | 320 | 30 | 0.0016 | 4.33 | 0 | 4.4 | 4.4 |
| | | 40 | 0.0204 | 5.75 | 0.0068 | 5.76 | 5.76 |
| | | 50 | 0.2648 | 7.25 | 0.0392 | 7.26 | 7.18 |
| | | 60 | 1.0758 | 8.64 | 0.2206 | 8.76 | 8.67 |
| | | 70 | 2.7075 | 9.91 | 0.6764 | 10.24 | 9.98 |

of these figures, let us give a more insight view about them by showing the blocking of the different classes of traffic as a function of the overall load. We have focused on the scenario with 160 FSs/link in both networks. Fig. 2 depicts the obtained results.

In general, we can see that the most important benefits of SSRSA against 1-SSRSA are experienced by those traffic classes requesting more bandwidth, as they can be split up and be more easily allocated. This is an interesting outcome indeed, as operators should expect the highest revenues from ultra-high bit rate super channels. In contrast, with more high bit-rate demands active in the network and less available resources, low bit-rate ones experience a slight increase on their blocking probability in some of the loads and scenarios. Nevertheless, this effect is almost non-perceptible and does not degrade the overall network performance in terms of blocked spectrum.

Regarding the average number of TSPs used per node with SSRSA, they are generally reduced when MF-TSPs are employed, since all parts of a split demand can be supported over a unique MF-TSP. However, note that such differences remain very small under realistic offered loads (e.g., offered loads leading to BBw $\leq 1\%$). This is because a low percentage of incoming demands needs to be split in such scenarios (around 1% of the total in average), which makes the MF-TSP capability to be considerably wasted most of the time.

In light of the above, we have additionally analyzed network CAPEX investments that would be incurred to implement SSA with either BV-TSPs or MF-TSPs in EON16 and DT networks, as a function of the relative cost of a MF-TSP against a BV-TSP. Parameter $\gamma$ is used for these purposes, so that $Cost_{MF-TSP} = \gamma \cdot Cost_{BV-TSP}$. Specifically,

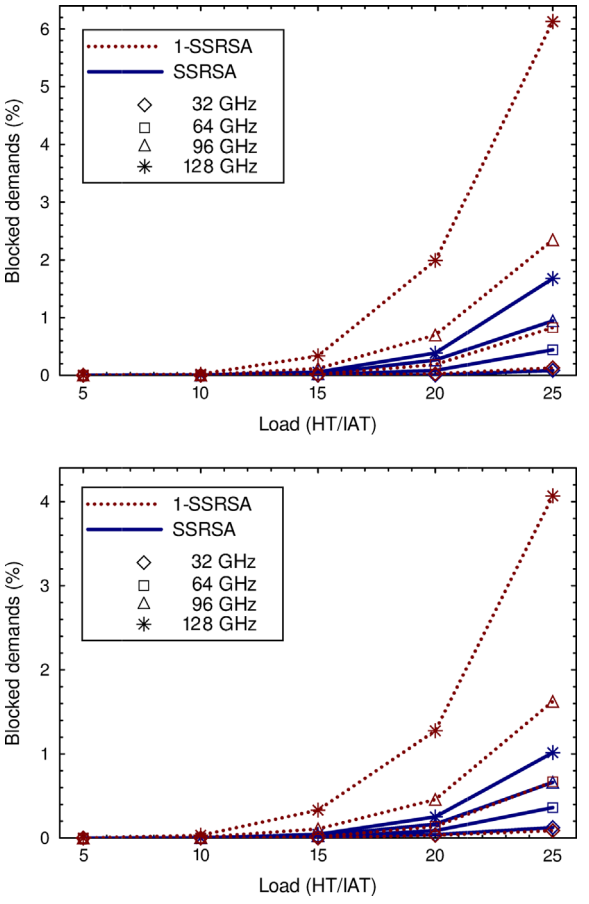


**Fig. 2.** Demand blocking for the different classes as a function of the load in EON16/160 (top) and DT/160 (bottom).

we have focused on the scenario with 320 FSs/link in both networks, as well as on two of the tested loads, namely, 60 and 70. The obtained results are shown in Fig. 3. The average network cost is calculated as Avg. TSPs/node $\times$ Nr TSPs $\times$ Cost of a TSP in both BV-TSP and MF-TSP implementations, setting $Cost_{BV-TSP}=1$ as the base unit of cost.

As observed, MF-TSPs are only cost-effective with $\gamma$ very close to 1, since demand splitting is infrequent under such a realistic offered loads leading to BBw $<1\%$. Conversely, assuming that $\gamma>1$ due to the inherently higher complexity of MF-TSPs compared to BV-TSPs, it is generally more appropriate to deploy a slightly overprovisioned number of BV-TSPs per node to perform SSA. For example, looking at Table 1 for the EON16 network and a load of 60, around 0.13 more BV-TSPs per node would be required to perform SSA, compared to a non-splitting scenario (1-SSRSA). In the same network, this value is increased to 0.66 for an offered load of 70.

Finally, in order to provide a more in depth performance evaluation of the SSRSA mechanism, we have extracted additional results. Throughout the following analysis, we have focused on the 160 FSs scenarios for both network topologies. The specific scenario details will be noted in every case. Firstly, since the presented

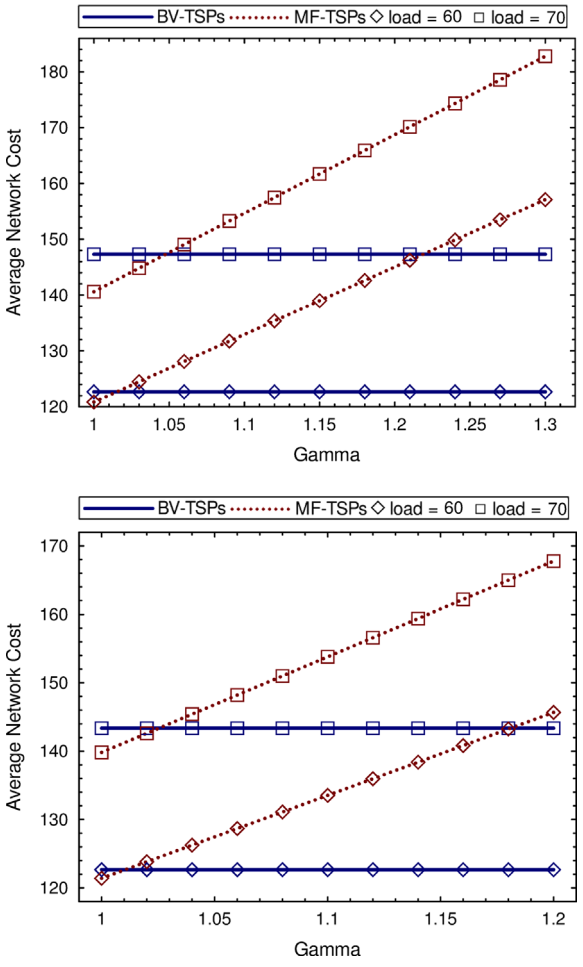


**Fig. 3.** Cost comparison in EON16/320 (top) and DT/320 (bottom).

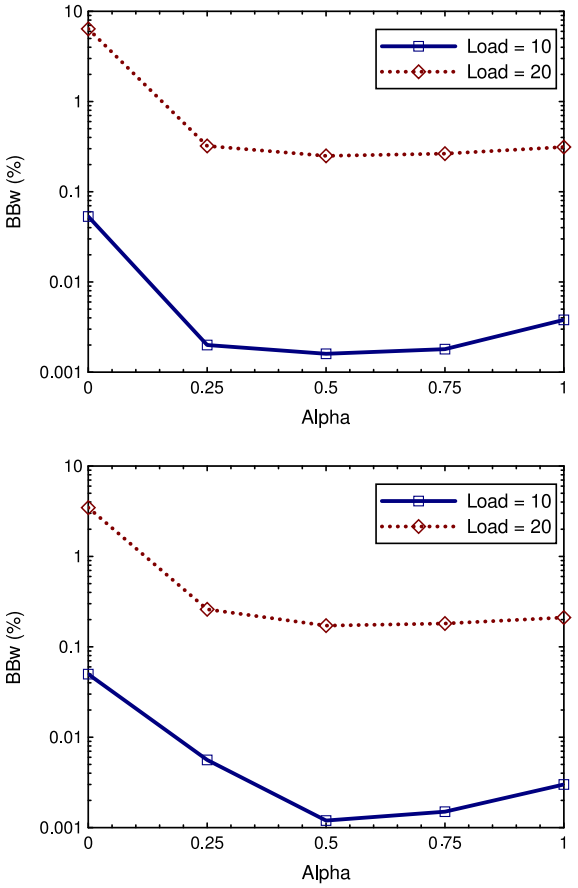


**Fig. 4.** Performance of SSRSA in EON16/160 (top) and DT/160 (bottom) as a function of $\alpha$.

mechanism has a multi-objective optimization goal, we evaluated how the BBw evolves depending on the value of the parameter $\alpha$. To this end, we have focused on two loads, namely 10 and 20, to see the impact of the value of $\alpha$ in various network load conditions. Fig. 4 depicts the obtained values.

It can be appreciated that the joint minimization of both the employed number of parts and the spectrum fragmentation leads to the best results in terms of BBw, as opposed to only focusing on one of the objectives ($\alpha=1$ or 0). Moreover, it can be seen that focusing only on the minimization of the spectrum fragmentation ($\alpha=0$) in a SS-enabled environment leads to a very poor performance. This phenomena happens due to the fact that, in order to minimize the spectrum fragmentation, the MILP formulation will divide the demand in many parts so as to fill as much spectral gaps as possible with aims of having the minimum number of contiguous busy spectrum portions. Furthermore, we can appreciate that for higher loads the impact of the value of alpha in the range $\geq 0.25$ is much less than in lower loads. This happens due to the fact that for higher loads, the lack of spectrum is more noticeable, so the model has less room to influence in the RSA choice for different values of $\alpha$.

For the following set of results, we analyzed how the BBw and the average number of TSPs per node (both in the

**Table 2**
Influence of the size of $P_d$.

| Scenario | | K=3 | | | K=4 | | | K=5 | | |
|---|---|---|---|---|---|---|---|---|---|---|
| **Network** | **Load** | **BBw** | **BV-TSPs** | **MF-TSPs** | **BBw** | **BV-TSPs** | **MF-TSPs** | **BBw** | **BV-TSPs** | **MF-TSPs** |
| EON16 | 5 | 0 | 0.69 | 0.69 | 0 | 0.68 | 0.68 | 0 | 0.68 | 0.68 |
| | 10 | 0.0016 | 1.3 | 1.3 | 0 | 1.31 | 1.31 | 0 | 1.31 | 1.31 |
| | 15 | 0.0319 | 1.93 | 1.93 | 0.0224 | 1.94 | 1.94 | 0.0136 | 1.93 | 1.93 |
| | 20 | 0.2499 | 2.57 | 2.55 | 0.1497 | 2.59 | 2.57 | 0.1277 | 2.58 | 2.56 |
| | 25 | 1.0503 | 3.26 | 3.18 | 0.7518 | 3.25 | 3.17 | 0.7425 | 3.27 | 3.19 |
| DT | 5 | 0 | 0.78 | 0.78 | 0 | 0.78 | 0.78 | 0 | 0.78 | 0.78 |
| | 10 | 0.0012 | 1.49 | 1.49 | 0.0015 | 1.5 | 1.5 | 0.0015 | 1.48 | 1.48 |
| | 15 | 0.0255 | 2.21 | 2.21 | 0.0144 | 2.21 | 2.21 | 0.0103 | 2.18 | 2.18 |
| | 20 | 0.1716 | 2.94 | 2.93 | 0.112 | 2.94 | 2.93 | 0.0753 | 2.9 | 2.89 |
| | 25 | 0.6913 | 3.67 | 3.61 | 0.4354 | 3.67 | 3.63 | 0.3605 | 3.67 | 3.62 |

BV-TSP and MF-TSP cases) evolves with the size of the candidate path set $P_d$. Table 2 depicts the obtained results. All the results have been extracted considering $\alpha=0.5$.

As expected, the percentage of BBw decreases with increasing values of $K$, with relative gains in the range 28–57% and 47–60% for the EON16 and DT network topologies, respectively, when increasing $K$ from 3 to 5 candidate paths. Regarding the average value of used transponders per node, the value remains more or less steady for all explored values of $K$ in general. Furthermore, despite the superior performance in terms of blocking of the SSRSA mechanism with higher values of $K$, although not shown, the execution times grow significantly. For example, we have experienced execution times in the range 270–450 ms for $K=3$ whereas for $K=5$ the execution times are in the range 370–720 ms. So, in such situation, for scenarios where demands require stringent times for assigning resources to them, it would be better to have a more limited set of candidate paths, due to the inferior computational requirements of the MILP formulation in such conditions.

Up to now, we have evaluated the presented mechanism considering that there are enough transponders at each node, i.e. no blocking due to the lack of them happens. Although this allowed us to evaluate which is the necessary number of both BV-TSPs and MF-TSPs per node for a maximum benefit of the SSA, in realistic network scenarios nodes are equipped with a limited set of transponders. In such conditions, this finite number of transponders may impact significantly on the number of demands that are blocked due to the lack of them, being this effect more notorious in the BV-TSP-based implementation.

To evaluate how the lack of transponders impacts on the overall blocking, we have executed additional experiments focusing on the BV-TSP-based implementation for both network topologies considering $K=3$ and $\alpha=0.5$ and a load equal to 20, comparing the case where no splitting is done (1SSRSA) against the case where splitting is allowed (SSRSA). We have set a number of transponders per node equal to the ceiling of the average number of transponders as depicted in Table 2 as the base case, e.g. for the EON16 network topology and a load of 20, this value would be equal to $\lceil 2.58 \rceil = 3$. Fig. 5 depicts the BBw as a function of $\Delta T$, where $\Delta T$ represents the number of additional transponders with respect to the base case.

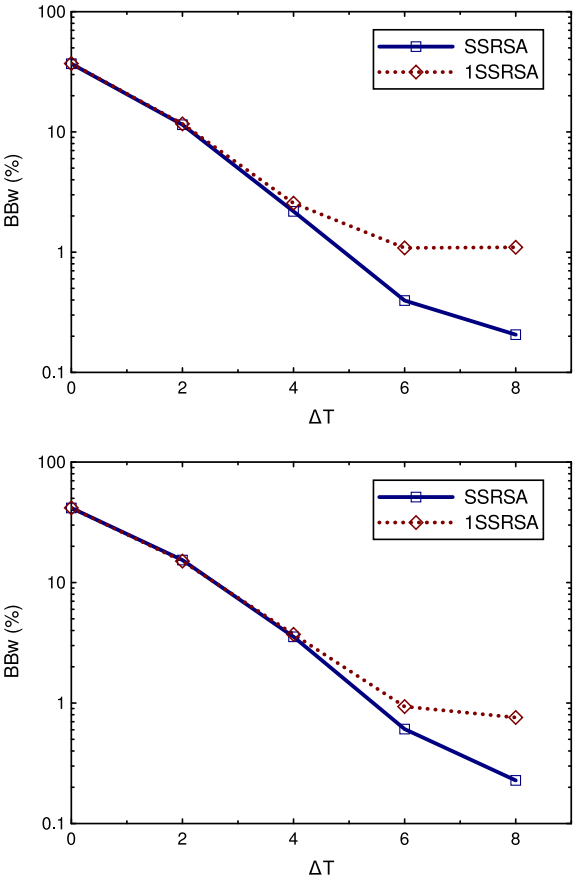


**Fig. 5.** Performance of SSRSA in EON16/160 (top) and DT/160 (bottom) as a function of $\Delta T$.

Following the previous example, $\Delta T=0$ means that 3 transponders are equipped per node whereas a value of $\Delta T=2$ means that 5 transponders are equipped per node.

We can see that the BBw dramatically increases in the base case where the number of transponders has been dimensioned according to the average extracted in previous analysis. This is mainly due to the burstiness of the traffic, that is, periods of time where the number of arrivals is superior to the mean arrival rate. In such situations, depending on the

number of parts that a demand is split, transponders at nodes can be rapidly exhausted, leading to blocking of future incoming demands. In fact, for $\Delta T = 0$, the main cause of blocking is due to the lack of transponders (around 98% in average for all tested scenarios whereas the rest is due to the lack of FSs). To achieve again blocking levels below 1% is necessary to equip each transponder with 6–8 extra transponders. In such situation, the blocking trends are inverted and the main cause of blocking becomes again the lack of free FSs (the blocking due to the lack of transponders is around 32%). Additionally, it can be appreciated that the overhead introduced by the splitting process in terms of necessary number of TSPs is very small, since both 1SSRSA and SSRSA need a very similar number of TSPs per node so as to regain sustainable blocking levels. Moreover, we can see that if no splitting is considered, there exists a point (around $\Delta T = 6$) where equipping extra TSPs to the nodes does not reduce anymore the blocking levels. This happens because, at this point, the lack of enough contiguous spectrum becomes the limiting factor, so deploying extra TSPs does not help on reducing the BBw. On the other hand, if the SSA is considered, we can see that it is possible to further reduce the BBw if enough TSPs are deployed, since the lack of enough contiguous spectrum is no longer a limiting factor.

Finally, as we commented during the description of H-SSRSA, SSRSA may suffer from scalability issues in larger network scenarios. Let us discuss in more depth the computational complexity of SSRSA. Looking back at its description, one can see that the number of binary variables of the MILP formulation is in the order of $\mathcal{O}(3K|F|)$ and the number of constraints is in the order of $\mathcal{O}((S_{min}+5)K|F|)$. It can be appreciated that its complexity is tightly related to the size of $F$. As for the value of $K$, this parameter can be tuned to find a trade-off between optimality and swiftness of the mechanism. However, little can be done regarding $|F|$, as it is an intrinsic characteristic of the network scenario. For this reason, we proposed H-SSRSA as an alternative mechanism to find good solutions at a lower computational cost. Fig. 6 depicts the comparison of H-SSRSA against SSRSA in terms of BBw as a function of the offered load. For these results, we considered $K=3$, $\alpha=0.5$ and no blocking due to the lack of TSPs.

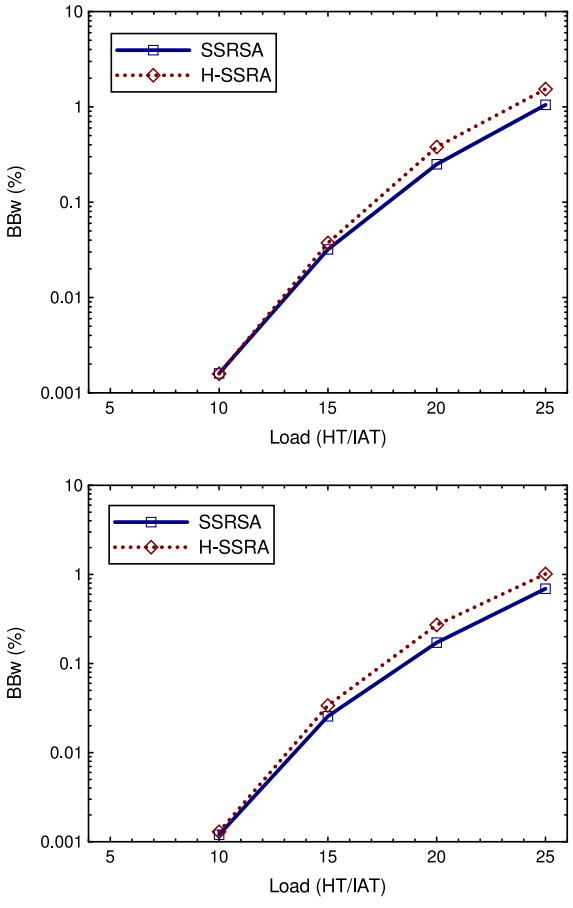


**Fig. 6.** H-SSRSA vs SSRSA in EON16/160 (top) and DT/160 (bottom).

It can be appreciated that H-SSRSA produces BBw figures very close to the ones obtained through SSRSA. As for the execution times that we experienced for both mechanisms, they are in the range 1.43–1.54 ms and 270–450 ms for H-SSRSA and SSRSA, respectively, in the 160 FSs scenarios, while they are in the range 1.33–1.74 ms and 340–730 ms for H-SSRSA and SSRSA, respectively, in the 320 FSs scenarios. It can be appreciated that, as pinpointed before, the execution times of SSRSA increase substantially as the size of $F$ grows up, while the execution times of H-SSRSA remain steady for all tested scenarios and more than one order of magnitude below those of SSRSA. For these reasons, H-SSRSA succeeds in its goal of providing near optimal solutions in much less time.

## 4. Conclusions

In this paper, we proposed a mechanism based on a formal MILP formulation for optimal SSA operation in dynamic elastic optical networks. Using this mechanism, we highlight the benefits of applying SSA, which can decrease the blocked bandwidth by one order of magnitude when compared against a standard RSA mechanism. We additionally presented a heuristic mechanism capable of producing good results in a very short time for network scenarios where scalability becomes an issue to be taken care of. Furthermore, we conclude that using MF-TSPs for SSA is only interesting if their cost remains close to that of the BV-TSPs.

## Acknowledgments

This work has been supported by the Government of Catalonia and the European Social Fund through a FI-AGAUR research scholarship grant and by the Spanish National project ELASTIC (TEC2011-27310).

## References

[1] O. Gerstel, M. Jinno, A. Lord, S.J.B. Yoo, Elastic optical networking: a new dawn for the optical layer? IEEE Commun. Mag. 50 (February (2)) (2012) s12–s20.
[2] M. Jinno, H. Takara, B. Kozicki, Y. Tsukishima, Y. Sone, S. Matsuoka, Spectrum-efficient and scalable elastic optical path network: architecture, benefits, and enabling technologies, IEEE Commun. Mag. 47 (November (11)) (2009) 66–73.

[3] M. Jinno, H. Takara, Y. Sone, Elastic optical path networking: enhancing network capacity and disaster survivability toward 1 Tbps era, in: 16th Opto-Electronics and Communications Conference (OECC 2011), July 2011.
[4] Y. Yin, K. Wen, D.J. Geisler, R. Liu, S.J.B. Yoo, Dynamic on-demand defragmentation in flexible bandwidth elastic optical networks, Opt. Express 20 (January (2)) (2012) 1798–1804.
[5] M. Zhang, Y. Yin, R. Proietti, Z. Zhu, S.J.B. Yoo, Spectrum defragmentation algorithms for elastic optical networks using hitless spectrum retuning techniques, in: Optical Fiber Communication Conference (OFC), March 2013.
[6] S. Syed, R. Rao, M. Sosa, B. Lu, A framework for control of flex grid networks, IETF draft, April 2012.
[7] I. Hussain, A. Dhillon, Z. Pan, M. Sosa, Generalized label for super-channel assignment on flexible grid, IETF draft, September 2012.
[8] M. Xia, R. Proietti, S. Dahlfort, S.J.B. Yoo, Split spectrum: a multi-channel approach to elastic optical networking, Opt. Express 20 (December (28)) (2012) 29143–29148.
[9] M. Jinno, H. Takara, Y. Sone, K. Yonenaga, A. Hirano, Multiflow optical transponder for efficient multilayer optical networking, IEEE Commun. Mag. 50 (May (5)) (2012) 56–65.
[10] A. Pagès, J. Perelló, S. Spadaro, Lightpath fragmentation for efficient spectrum utilization in dynamic elastic optical networks, in: 16th International Conference on Optical Networking Design and Modeling (ONDM 2012), April 2012.
[11] Z. Zhu, W. Lu, L. Zhang, N. Ansari, Dynamic service provisioning in elastic optical networks with hybrid single-/multi-path routing, J. Lightwave Technol. 31 (January (1)) (2013) 15–22.
[12] W. Lu, X. Zhou, L. Gong, M. Zhang, Z. Zhu, Dynamic multi-path service provisioning under differential delay constraint in elastic optical networks, IEEE Commun. Lett. 17 (January (1)) (2013) 158–161.
[13] X. Cheny, A. Jukany, A. Gumaste, Multipath de-fragmentation: achieving better spectral efficiency in elastic optical path networks, in: 32nd IEEE International Conference on Computer Communications (INFOCOM 2013), April 2013.
[14] N. Amaya, M. Irfan, G. Zervas, K. Banias, M. Garrich, I. Henning, D. Simeonidou, Y.R. Zhou, A. Lord, K. Smith, V.J.F. Rancano, S. Liu, P. Petropoulos, D.J. Richardson, Gridless optical networking field trial: flexible spectrum switching, defragmentation and transport of 10G/40G/100G/555G over 620-km field fiber, in: 37th European Conference and Exhibition on Optical Communication (ECOC 2011), September 2011.
[15] K. Walkowiak, M. Klinkowski, Joint anycast and unicast routing for elastic optical networks: modeling and optimization, in: IEEE International Conference on Communications (ICC) 2013, June 2013.
[16] S. De Maesschalck, D. Colle, I. Lievens, M. Pickavet, P. Demeester, C. Mauz, M. Jaeger, R. Inkret, B. Mikac, J. Derkacz, Pan-European optical transport networks: an availability-based comparison, Photonic Netw. Commun. 5 (May (3)) (2003) 203–225.
[17] F. Agraz, S. Azodolmolky, M. Angelou, J. Perelló, L. Velasco, S. Spadaro, A. Francescon, C.V. Saradhi, Y. Pointurier, P. Kokkinos, E. Varvarigos, M. Gunkel, I. Tomkos, Experimental demonstration of centralized and distributed impairment-aware control plane schemes for dynamic transparent optical networks, in: Optical Fiber Communication Conference (OFC), March 2010.